XMM-Newton CCF Release Note

XMM-CCF-REL-275

Modification of the RGS line-spread function

A.M.T. Pollock

December 17, 2011

1 CCF components

Name of CCF	VALDATE	List of Blocks changed	XSCS flag
RGS1_LINESPREADFUNC_0005	2001-01-01T00:00:00	FIGURE	NO
RGS2_LINESPREADFUNC_0005	2001-01-01T00:00:00	FIGURE	NO

2 Changes

Measurements of the positions and widths of lines as accurate as possible is an important calibration requirement of the high-resolution RGS. A robust calibration model of the instrumental response, allows observers to concentrate on the instrinsic shapes of lines in cosmic sources and make full use of the resolving power available to study blends. Such calibration measurements are best made by modelling the observed distributions of events in narrow lines in tools such as XSPEC using the detailed description of the line-spread function, or LSF, encoded in the response matrix. The success of this procedure may partly be judged by how well qualitatively and quantitatively the model fits observed lines.

The LSF model is complex, containing many components. Ton Raassen from SRON Utrecht has investigated the effect of varying parameters of some components and proposed new LSFs with modified parameters describing the non-uniformity of alignments of the ensemble of grating elements known as the `FIGURE` distribution. In both RGS instruments, this is modelled as the combination of three Gaussian distributions, designated 1, 2, 3. Raassen proposes the following modifications:

- RGS1 Gaussian 2 `AMPLITUDE` = `AMPLITUDE`/0.8 and `SIGMA` = `SIGMA` $\times$ 0.8
- RGS2 Exchange signs of the `CENTER`s of Gaussians 1 and 2

Old and new values of the `FIGURE` gaussian parameters are shown in Table 1.

CCF	AMPLITUDE .	CENTER 10^{-5} rad	SIGMA 10^{-5} rad
RGS1_LINESPREADFUNC_000[45].CCF			
0004	234.8095	+5.081369	0.6148746
0005	234.8095	+5.081369	0.6148746
0004	**875.5271**	+3.629649	**0.7568045**
0005	**1094.4089**	+3.629649	**0.6054436**
0004	119.0044	+2.201019	0.4183546
0005	119.0044	+2.201019	0.4183546
RGS2_LINESPREADFUNC_000[45].CCF			
0004	36.76106	+**1.539544**	2.59085
0005	36.76106	−**1.539544**	2.59085
0004	195.6043	−**1.998606**	0.8578722
0005	195.6043	+**1.998606**	0.8578722
0004	460.6941	+0.5485315	1.26581
0004	460.6941	+0.5485315	1.26581

Table 1: Parameters of the 3 Gaussians used to describe the RGS gratings `FIGURE` distributions arranged to emphasise the differences devised by Raassen to improve the quality of models of RGS emission lines.

3 Test procedures & results

Old and new LSF CCFs were compared through the fit statistics of XSPEC models of the coronal sources AB Dor, Capella, HR 1099 and Procyon for two sets of RGS RMFs generated by `rgsproc` in SASv11 with

- `LSF_0004` RGS[12]_LINESPREADFUNC CCFs public version
- `LSF_0005` RGS[12]_LINESPREADFUNC CCFs new version

The models used were those of the 2007 coronal-line survey [1], although the new analysis incorporates CCF changes since then, notably the time-variable effective area, and more recent data, giving 72 spectra up to 2011-01-02.

The global models contain as many narrow lines as judged necessary in 2007 to model the entire spectrum for the purpose of calculating a single mean line shift. For XSPEC analysis, RMFs were calculated with 20,000 rows. This global comparison is shown in Figure 1. As in 2007, a few solutions were poor with $C > 20,000$, especially for Capella because of pile-up and the absence of NiXIX and NiXX from the model. In order to avoid spurious local minima in parameter space, solutions were "shaken" in 1st order parameter space. XSPEC analysis of a typical spectrum took about 24 hours on the grid.

Overall, the ΔC statistical gain in these global fits was modest, although this probably reflects the difficulty of deriving a model that works at all RGS wavelengths. Therefore, further local model comparisons were made separately in RGS1 and RGS2 in 1st order in narrow $\pm$0.25Å intervals around strong lines. This gives the advantage of imposing fewer contraints on the level of nearby lines and continuum, allowing attention to be focussed on the lines themselves. At the 10mÅ spectrum bin width, these local models covered 49 bins. The statistical gain of these comparisons is shown in Figure 2. Many fits were improved with the new LSFs although some remain poor as judged by the value of the C-statistic. A good fit would have C$\approx$NBINS.

The number of counts detected in a line in an individual observation is often small and thus subject to numerical fluctuations. An effective way to judge the success of a model is to combine data where possible. Background-subtracted data and models of individual local line fits in the sample stars were stacked in order to compare more sensitively the quality of the alternative model LSFs. Figures 3 and 4 show results for AB Dor with C-statistic calculations given in Table 2. The fits provided by the new `RGS[12]_LINESPREADFUNC_0005.CCF`s are consistently better, including the line core. In the best example, the stack C-statistic of OVIII λ18.967 in RGS2 was reduced from 494.6 to 126.7, approaching a formally acceptable value.

	RGS1			RGS2		
	C(0004)	C(0005)	NBINS	C(0004)	C(0005)	NBINS
CVI λ33.734	72.1	64.0	49	126.8	110.7	49
OVII λ21.602	115.3	99.9	49	...	...	...
OVIII λ18.967	639.6	549.4	49	494.6	126.7	49
FeXVII λ16.778	147.6	129.5	49	175.4	111.3	49
FeXVII λ15.015	141.2	121.8	49	162.2	155.2	49
NeX λ12.132	...	...	...	180.2	135.9	49

Table 2: Values of the C-statistic for fits including those shown in Figures 3 and 4 of stacked models to stacked data of strong, reasonably isolated lines in 34 observations of AB Dor. The models provided by the new `RGS[12]_LINESPREADFUNC_0005.CCF`s are consistently better. A statistically acceptable model would have C$\approx$NBINS. The missing RGS1 CCD7 and RGS2 CCD4 account for the absense of a second measurement of OVII λ21.602 and NeX λ12.132.

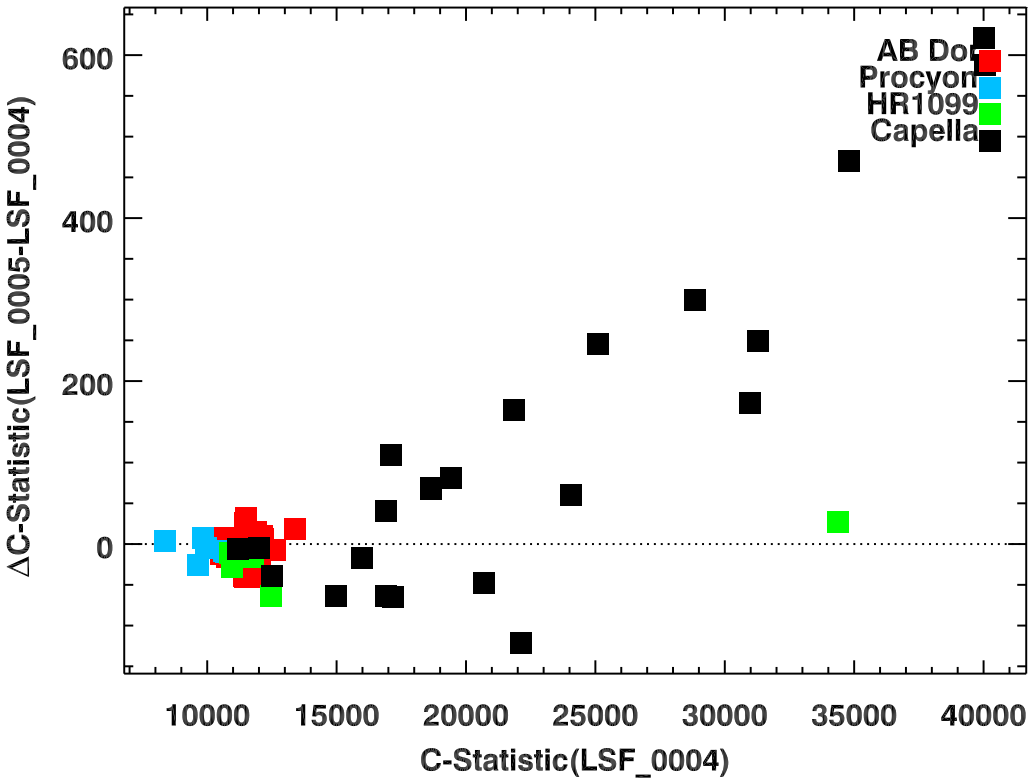

Figure 1: C-statistic differences between global multiple narrow-line models calculated with the new `LSF_0005` and old `LSF_0004`. For typical "acceptable" combined RGS1 and RGS2 C-statistic values of 10,000-20,000, the new LSFs give generally better fits with $\Delta C \leq -70$.

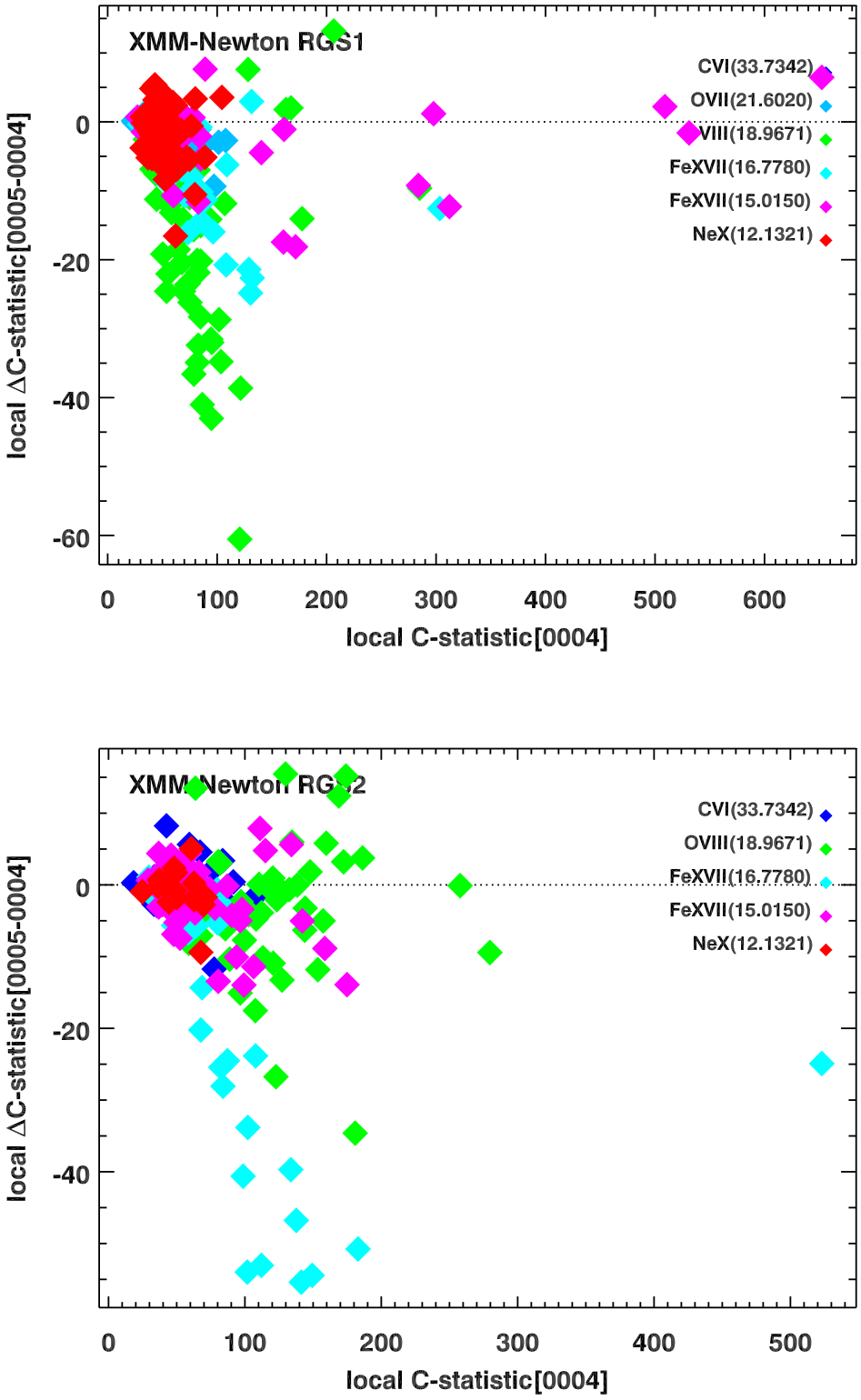

Figure 2: Statistical gain for local 49-bin models of individual lines with `LSF_0004` and `LSF_0005` for RGS1 above and RGS2 below.

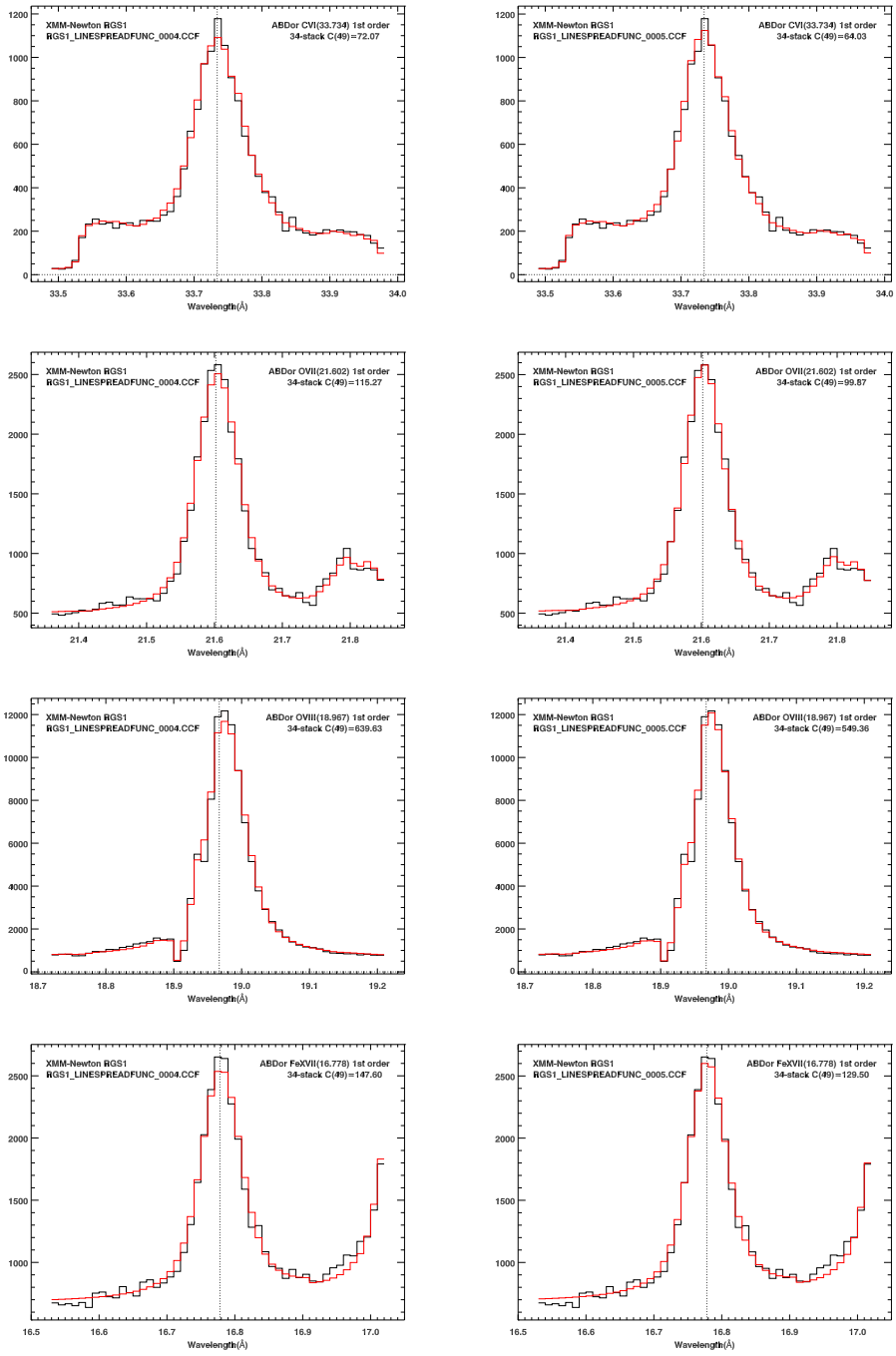

Figure 3: Stacked data (black) and models (red) of 34 RGS1 observations of AB Dor within 0.25Å of the strong emission lines from top to bottom of CVI λ33.734, OVII λ21.602, OVIII λ18.967 and FeXVII λ16.778. Models calculated with the current public `RGS1_LINESPREADFUNC_0004.CCF` are on the left and the new `RGS1_LINESPREADFUNC_0005.CCF` on the right. Data on both sides are identical. The C-statistics shown allow direct comparison of of the two alternative LSFs and demonstrate the superiority of the new version. The vertical dotted lines shows the laboratory wavelengths.

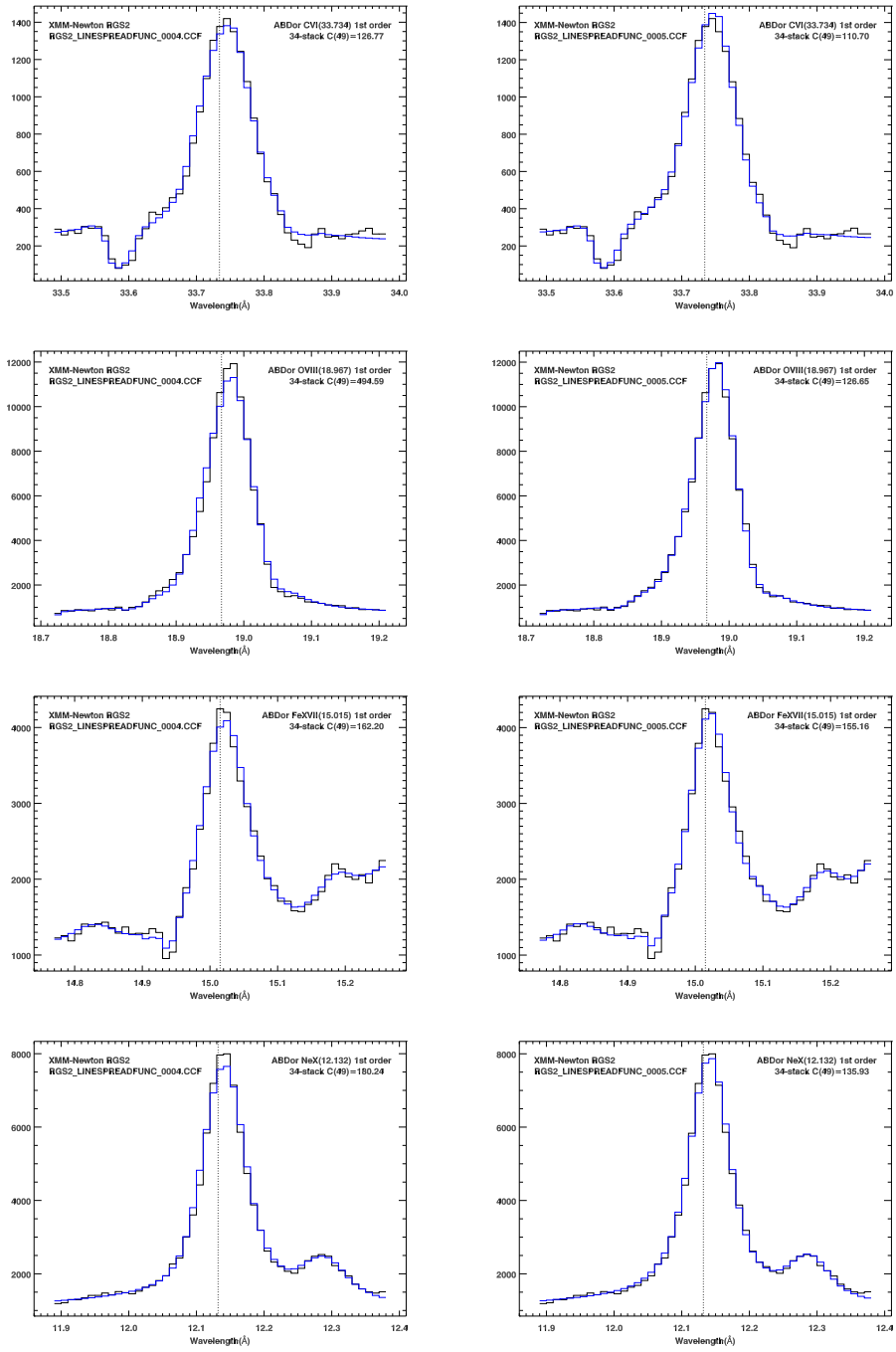

Figure 4: Stacked data (black) and models (blue) of 34 RGS2 observations of AB Dor within 0.25Å of the strong emission lines from top to bottom of CVI λ33.734, OVIII λ18.967 FeXVII λ15.015 and NeX λ12.132. Models calculated with the current public `RGS2_LINESPREADFUNC_0004.CCF` are on the left and the new `RGS2_LINESPREADFUNC_0005.CCF` on the right. Data on both sides are identical. The C-statistics shown allow direct comparison of of the two alternative LSFs and demonstrate the superiority of the new version. The vertical dotted lines shows the laboratory wavelengths.

4 Estimated Scientific Quality

The general improvement in the statistical quality of the stacked models and data bring within reach the prospect of a statistically acceptable calibration model of the RGS LSFs.

The change in shape of the new LSFs causes significantly different wavelength estimates in RGS2 in particular. As shown in Figure 5, RGS1 wavelength estimates are essentially unchanged, while RGS2 estimates differ by -2.0 mÅ between old and new. Figure 6 shows fitted global line shifts, $\Delta\lambda = (\lambda - \lambda_{\rm lab})$ for RGS1 and RGS2 for the old and new CCFs showing that the misalignment between RGS1 and RGS2 wavelength scales is smaller with the new LSFs.

While the new LSFs improve the quality of RGS models of narrow emission lines, there is still room for improvement. A more thorough exploration is required of the complex parameter space spanned by the extensive set of values that specify the calibration model of the LSF. These CCF data are used by the CAL to calculate a single wavelength-independent basis function $\mathcal{L}(\Delta\beta)$, where β is the dispersion angle. Figure 7 shows the corresponding observed composite profile calculated from an extensive set of lines from all AB Dor data in comparison with the `FIGURE` distributions of the old and new LSFs. The change in RGS2 shape is at least qualitatively consistent with the shift in wavelength estimates.

5 Expected Updates

Investigations are underway towards a complete understanding of how the LSF is used by `rgsrmfgen` in order to devise a statistically acceptable model LSF.

References

[1] A survey of lines in coronal sources for the RGS wavelength scale, XMM-SOC-CAL-TN-79 `http://xmm.esac.esa.int/docs/documents/CAL-TN-0079-1-0`

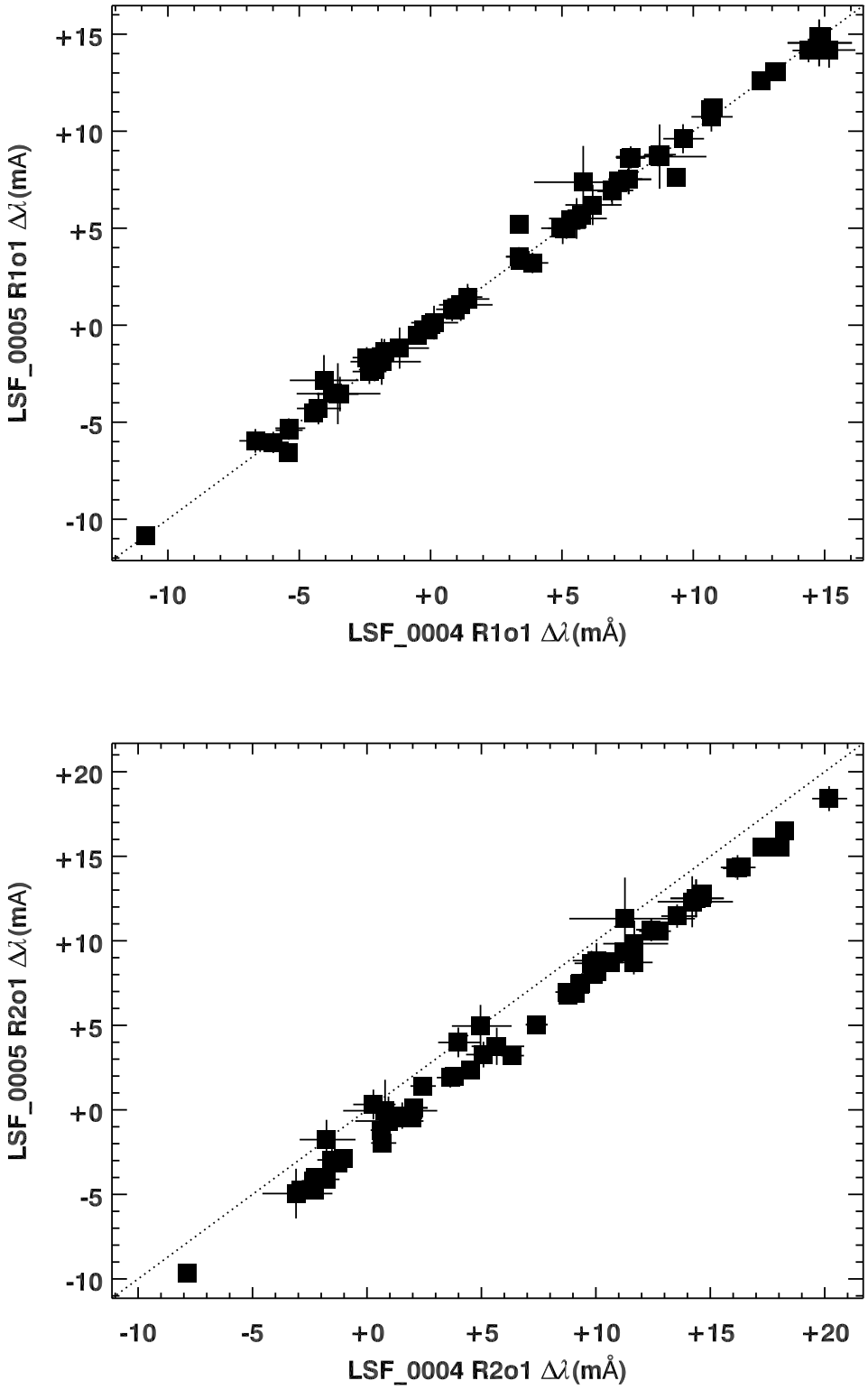

Figure 5: Global 1st-order line shifts, $\Delta\lambda = (\lambda - \lambda_{\rm lab})$, for spectra modelled with `LSF_0004` and `LSF_0005` for RGS1 above and RGS2 below.

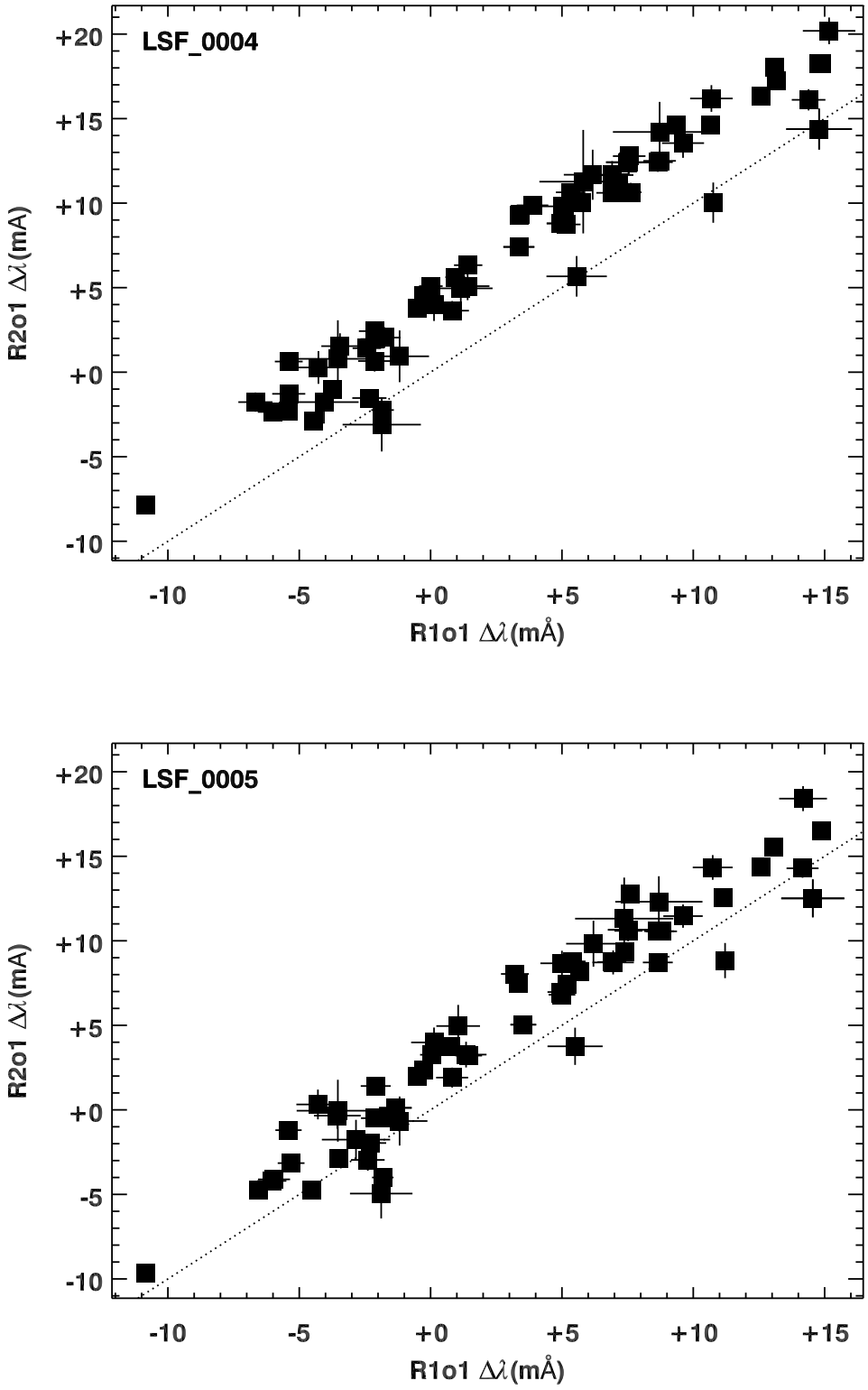

Figure 6: Global 1st-order line shifts, $\Delta\lambda = (\lambda - \lambda_{\rm lab})$, for spectra of RGS1 and RGS2 for the current `LSF_0004` above and the proposed `LSF_0005` below. The familiar correlation between the shifts estimated independently for RGS1 and RGS2 testifies to known systematic errors.

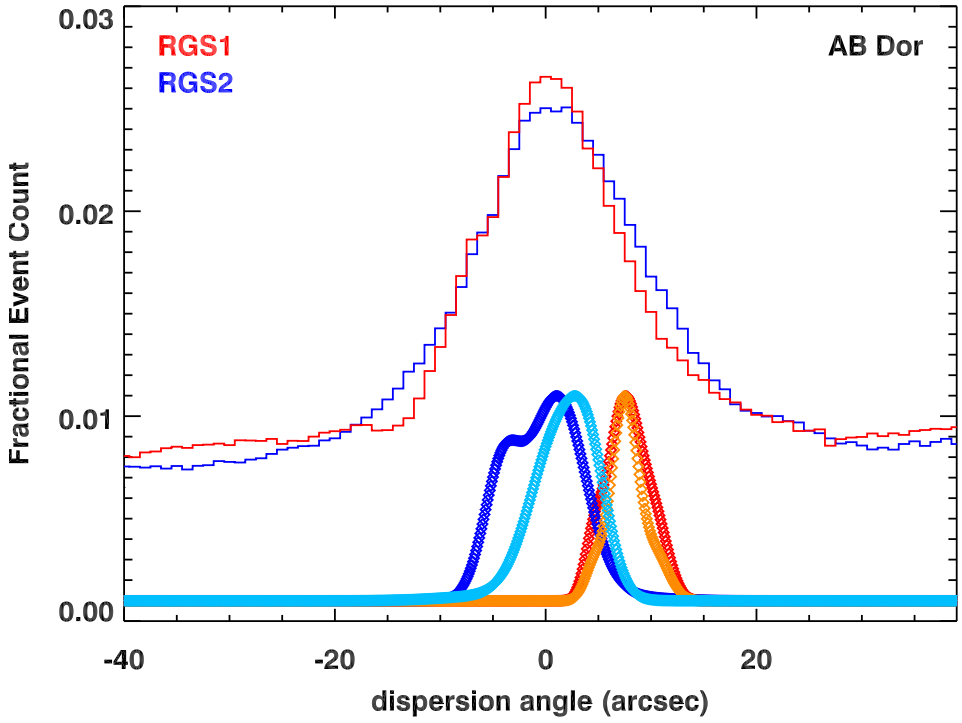

Figure 7: The upper curves show the composite dispersion-angle profiles of RGS1 and RGS2 data for the emission lines of AB Dor. In addition to instrumental calibration, these observed profiles have also been affected by systematic errors probably related to the thermal state of the instrument and heliospheric variations that are not yet taken into acccount. The points below show the `FIGURE` distributions calculated from the combination of 3 Gaussians that are the subject of the CCF change: `LSF_0004` and `LSF_0005` are shown in red and orange, respectively, for RGS1 and in dark and light blue for RGS2. These distributions have not been shifted along the dispersion axis and reflect a real difference in the symmetry of one component of the complex LSF model.